HYDROSTATIC PRESSURE INDUCED DUCTILITY TRANSITIONS IN PURE BISMUTH AND TIN–BISMUTH ALLOYS*

PETER V. DEMBOWSKI†, JOSEPH PEPE‡ and THOMAS E. DAVIDSON§

The mechanical behavior of pure (99.999%) bismuth and tin–bismuth alloys of various compositions has been observed over a range of superimposed hydrostatic pressures. Results indicate that maxima in ductility (as measured by percent reduction in each at the fracture surface) in specimens tested at atmospheric pressure occur at compositions bordering pure tin and the eutectic compositions. At sufficiently high pressures all compositions failed by rupture, i.e. necking to virtually 100 per cent RA. For pure bismuth, pressure was observed to retard failure due to the formation of cracks at twin-grain boundary interactions; this result was consistent with the hypothesis that the effect of pressure is to shift the mode of crack propagation by decreasing the normal tensile component of stress acting on a crack.

TRANSITIONS DE DUCTILITE DUES A UNE PRESSION HYDROSTATIQUE DANS LE BISMUTH PUR ET DANS LES ALLIAGES ETAIN–BISMUTH

Les auteurs ont étudié les propriétés mécaniques du bismuth pur (99,999%) et de divers alliages étain–bismuth en présence de pressions hydrostatiques. Les résultats indiquent que pour les échantillons déformés à la pression atmosphérique, la ductilité maximale (mesurée par la réduction de section en % à la surface de rupture) se produit pour des compositions voisines de l'étain pur et des eutectiques. Pour des pressions suffisantes, tous les alliages cassent avec des strictions de pratiquement 100%. Dans le bismuth pur, la pression retarde la cassure due à la formation de fissures aux intersections de joints de grains et de joints de macle; ce résultat s'accorde avec l'hypothèse que la pression change le mode de propagation d'une fissure en diminuant la contrainte normale agissant sur elle.

DUKTILITÄTS-ÜBERGÄNGE IN REINEM WISMUT UND IN ZINN–WISMUT-LEGIERUNGEN UNTER EINEM HYDROSTATISCHEN DRUCK

Das mechanische Verhalten von reinem Wismut (99,999%) und von Zinn–Wismut–Legierungen wurde bei verschiedenen hydrostatischen Drucken beobachtet. Die Ergebnisse zeigen, daß Duktilitätsmaxima (Meßgröße ist prozentuale Reduzierung an Bruchfläche) in den bei Atmosphärendruck untersuchten Proben in nahezu reinem Zinn und in Proben mit nahezu eutektischer Zusammensetzung auftreten. Bei genügend hohen Drucken kamen Proben aller Zusammensetzungen zum Bruch, d.h. Halsbildung bis virtuell 100% RA. In reinem Wismut verzögert hydrostatischer Druck den Bruch aufgrund einer Rißbildung an Zwilling-Korngrenzen-Schnittlinien. Dieses Ergebnis ist in Übereinstimmung mit der Hypothese, daß der Druck den Rißausbreitungsmechanismus durch ein Verminderung der normalen auf den Riß wirkenden Zugspannungskomponente verschiebt.

INTRODUCTION

In general, it has been observed that ductility, measured by either percent reduction in area at the fracture surface or the natural strain to fracture ($\ln (A_0/A_f)$), is increased by a superimposed hydrostatic pressure. The ductility pressure function can be either linear with a characteristic slope,[1,2] non-linear,[3,4] or abruptly increasing within a limited region of pressure.[5–7] A comprehensive review of the effects of pressure on mechanical properties of materials and techniques for determining these effects will not be attempted here, and the reader is referred to a review by Brandes[8] for this information.

Most investigations concerning the effects of pressure on the ductility of materials have been limited to single phase alloys or pure materials. In this current study, a two phase alloy, wherin the two phases exhibit marked differences in intrinsic ductility and pressure response is examined. Chosen for study was the tin–bismuth alloy system. Here the nature of the system is such that there is little room temperature solid solubility and the existence of a eutectic reaction permits variation of mixture morphology.

Prior work[9] has shown that bismuth undergoes an abrupt increase in ductility over a narrow pressure range. It has also been reported[10] that a 50 at.% Sn–50 at.% Bi alloy shows a similar abrupt transition, but that further increases in pressure above the transition pressure results in a decrease in ductility. Such a phenomena is contrary to the observed behavior of many other materials and inconsistent with proposed explanations of the pressure effect on ductility.

Reported herein is the response of ductility to pressure for several Sn–Bi compositions and microstructures. The pressure effects upon ductility are interpreted in terms of the fracture modes observed.

* Received January 10, 1974; revised February 28, 1974.

† Advanced Engineering Division, Benet Weapons Laboratory, Watervliet Arsenal, Watervliet, New York, U.S.A.

‡ Materials Engineering Division, Benet Weapons Laboratory, Watervliet Arsenal, Watervliet, New York, U.S.A.

§ Materials Engineering Division, Benet Weapons Laboratory, Watervliet Arsenal, Watervliet, New York, U.S.A.

TABLE 1. Fabrication conditions

Composition	Method extrusion	Temperature	Post extrusion treatment	Lubricant
100% Bi	Hot	150°C	a. Air cooled b. Water quenched	None
9% Sn–bal Bi	Hot	150°C	Air Cooled	None
30% Sn–bal Bi	Hydrostatic	Ambient	None	Pb–MoS_2
42% Sn–bal Bi	Hydrostatic	Ambient	None	None
75% Sn–bal Bi	Hydrostatic	Ambient	None	Pb–MoS_2
90% Sn–bal Bi	Hydrostatic	Ambient	None	None

Note: Virtually no change in intercept grain size as a function of cooling rate was observed in pure bismuth.

MATERIALS AND PROCEDURE

The bismuth and tin used in the fabrication of the alloy compositions were reagent grade stock; the nominal purity level of the former being 99.8 per cent Bi and the latter 99.9 per cent Sn. The material used for investigating the pressure–ductility response of pure bismuth was of high purity (99.999 per cent) $\frac{1}{2}$ in. polycrystalline bar stock. Alloys were prepared by melting in a Pyrex crucible open to the atmosphere and using $SnCl_2$ as a flux. Wherever possible, bismuth was added to the tin to minimize oxidation. Fabrication conditions for bar stock are given in Table 1 and the specimen annealing schedule in Table 2. All temperatures listed were held to within ± 2°C. All specimens were packed in fire clay powder prior to annealing.

Specimens were cylindrical in shape, having a nominal gauge length of 0.562 in. (the shoulder to shoulder distance) and diameters of either 0.160 (pure bismuth) or 0.090 in. (tin–bismuth alloys). The apparatus used in the course of the investigation was a 30 kb Bridgman–Birch hydrostatic system which has been previously described;[7] pressure measurement was accomplished through the use of a manganin wire transducer used in conjunction with a Foxboro recorder. The estimated error in pressure measurement was ± 2 per cent.

Extension of the specimen was accomplished through use of the fixture shown in Fig. 1. Tensile force is introduced into the specimen by the advance of the main piston into the pressure cavity, with this motion in turn transmitted into the specimen by two movable legs. The other two legs are stationary and bear against the bottom closure of the high pressure cavity, thereby fixing the position of one end of the specimen. Since straining of the specimen is accomplished by the advance of the piston into the high pressure cavity, the tests are not isobaric and an increase in pressure occurs as the specimen is extended. In reporting data the pressure at fracture is plotted. Crosshead movement was estimated from a record of piston displacement and was maintained at a rate of 0.05 in/min. All tests were performed at ambient temperatures.

Due to the relative softness of the materials used, mounting specimens for metallographic examination in an epoxy compound (Hysol) was adequate to insure reasonably good edge retention. Pure bismuth was examined in the as polished condition using polarized light and the Sn–Bi alloys were examined in either the as polished condition, or were etched using a solution of 10 ml hydrochloric acid and 0.5 g chromic acid in 250 ml of water prior to viewing. Electron micrographs were prepared using a two stage replication technique employing chromium as a shadowing material.

TABLE 2. Annealing schedule for Bi and Sn–Bi alloys

Composition	Condition prior to annealing	Annealing schedule	Comments
100% Bi	Hot extruded and air cooled Hot extruded and water quenched	None None	If the extrusion temp. is 66C, the grain dia immediately after extrusion is very small and increases to approximately 12.5 mm in 24 hr
9% Sn–bal Bi	Hot extruded and air cooled	ST	—
30% Sn–bal Bi	Hydrostatically extruded	(a) None (b) ST	Pb–MoS_2 coating not removed
42% Sn–bal Bi	do.	132C for 25 hr, air cooled	—
75% Sn–bal Bi	do.	ST	—
90% Sn–bal Bi	do.	ST	—

Note: "ST" is defined as heating at 120C for 235 hr, quenching into water at 0°C, upquenching to 24C for 14 hr and a second upquench to 66C for 4 hr, followed by air cooling to room temperature.

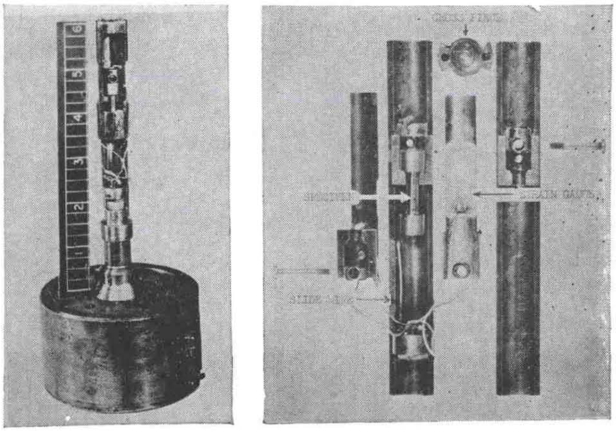

FIG. 1. High pressure tensile test fixture.

RESULTS

Effect of pressure on ductility and fracture appearance

The effects of pressure on the various materials examined is summarized in the pressure versus reduction in area plots shown in Figs. 2(a–e). For simplicity, each of the materials will be separately considered.

Pure bismuth

The effect of superimposed pressure upon the tensile ductility of pure bismuth is shown in Fig. 2(a), along with the data of Pugh.(4) It should be noted that a sharp ductility transition is observed for this material at a particular pressure which will be defined as the Brittle to Ductile Transition Pressure (BDTP) and will correspond to the lowest pressure

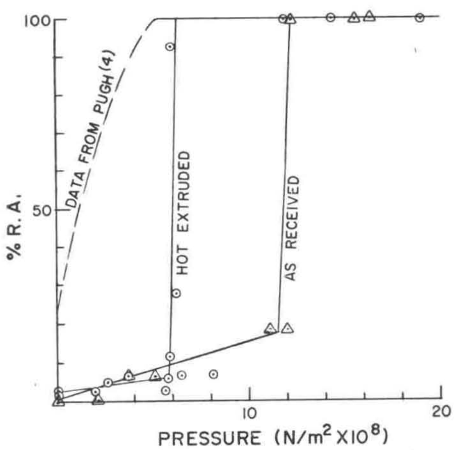

FIGURE 2A

FIG. 2(a). Pressure–ductility curve for 100% Bi, comparing results for columnar (as cast) and equiaxed (extruded) microstructures to data derived from results reported by Pugh.(4)

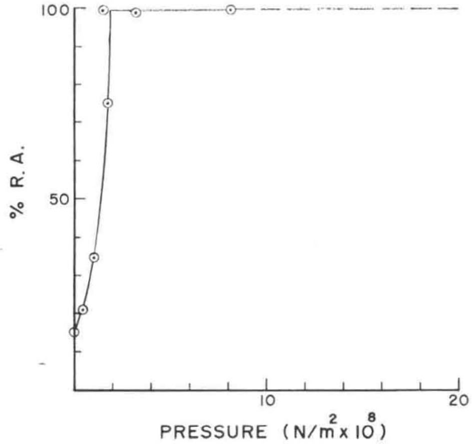

FIG. 2(b). Pressure–ductility curve for a 90% Sn–bal Bi alloy.

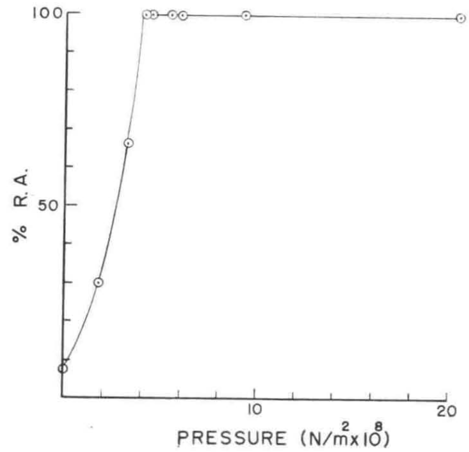

FIG. 2(c). Pressure–ductility curve for a 75% Sn–bal Bi alloy.

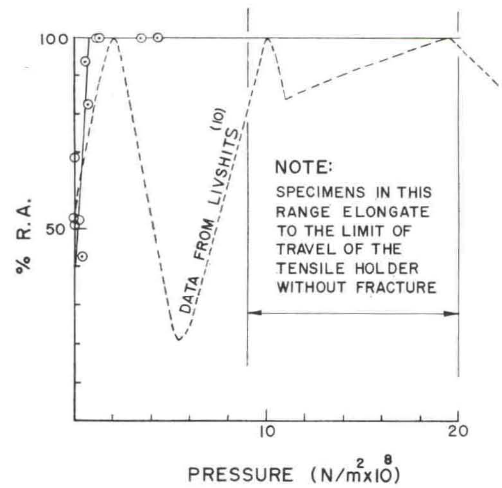

FIG. 2(d). Pressure–ductility curve for a 42% SN-bal Bi alloy. Results derived from data reported by Livshits *et al.*(10) are shown for comparison.

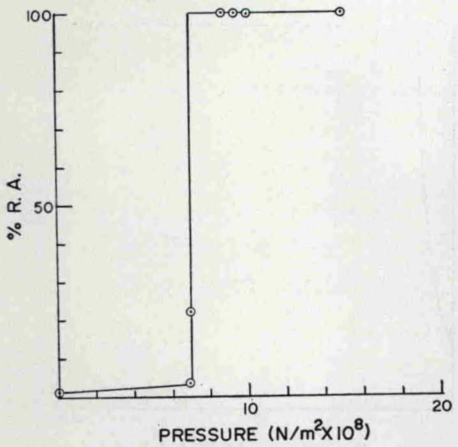

FIG. 2(e). Pressure–ductility curve for a 9% Sn–bal Bi alloy.

FIG. 3. The appearance of the fracture surface of a pure bismuth specimen which fractured at 5.0×10^8 N/m^2. $3250\times$

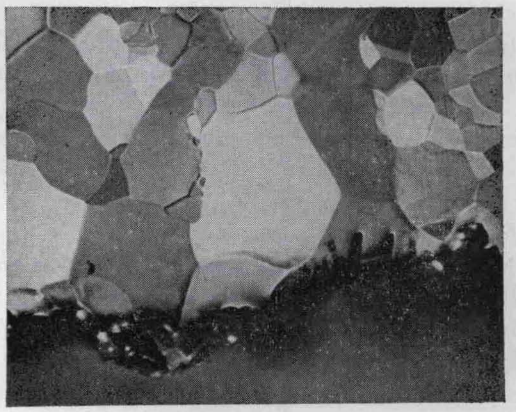

FIG. 4(a). The microstructure of pure bismuth specimens tested to failure at atmospheric pressure. $50\times$, Unetched, Polarized Light.

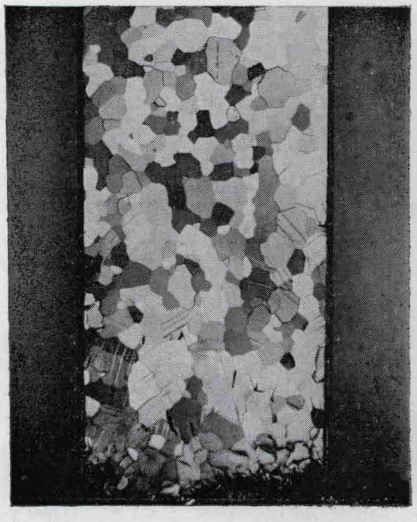

FIG. 4(b). The microstructure of pure bismuth specimens tested to failure at atmospheric pressure, $15\times$. Unetched, Polarized Light.

resulting in virtually 100 per cent reduction in area. It should be noted that the BDTP is highly structure sensitive. The BDTP was observed to be approximately 6×10^8N/m^2 (6 kb-) when the structure consisted of equiaxed grains with an average grain boundary intercept distance of 0.33 mm. However, when the material was in the as-cast condition the BDTP was observed to be approximately 11.5×10^8N/m^2 (11.5 kb). In addition to being cast, this material had a significantly larger grain size, the average grain size being as much as one-half the specimen diameter or approximately 1.15 mm in some areas of the specimen. Referring to Figs. 3 and 4(a), the fracture mode below the transition pressure is transgranular cleavage. Numerous stable microcracks are present behind the fracture surface of a tensile specimen fractured at atmospheric pressure and the number of mechanical twins increased as the fracture surface is approached (Fig. 4b). As can be seen by comparing Fig. 7(a) with 7(b), the macroscopic fracture mode changes with pressure from a flat crystalline type to ductile rupture.

Careful examination of the region in the vicinity of the tensile fracture surface revealed that the predominant mechanism of crack nucleation was the intersection of twins with grain boundaries as seen in Figs. 5(a) and (b). Although the predominant crack in Fig. 5(b) is not apparently associated with a twin-grain boundary interaction, this is simply a manifestation of the polished surface not intersecting the point of crack nucleation as is schematically shown in Fig. 6.

Increasing the level of superimposed pressure towards the BDTP results in a small increase in ductility. The resultant mechanical twin density is increased, but there is a decrease in the number of microcracks

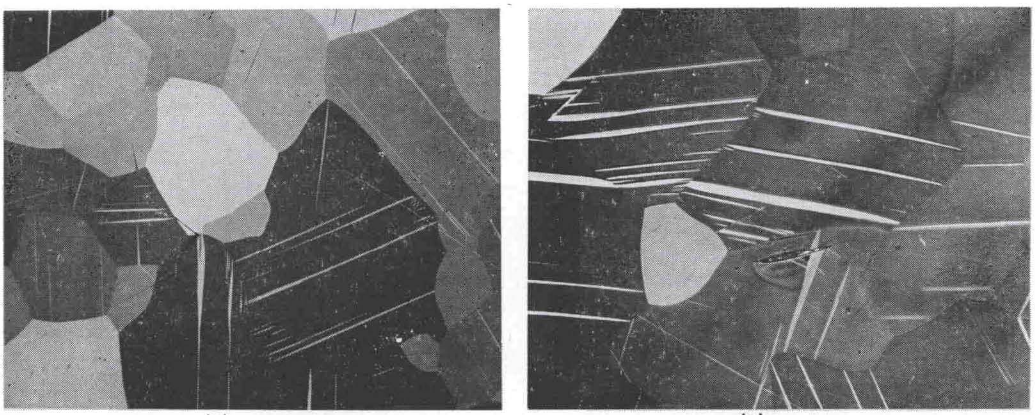

FIG. 5. The microstructure of a pure bismuth specimen tested to failure at atmospheric pressure showing: (a) Cracks formed by the intersection of ~~turns~~ TWINS with grain boundaries (75 ×, Unetched, Polarized Light), and (b) Twin-crack pairs felt to nucleate below the plane of polish by the mechanism outlined in Fig. 6. (100 ×, Unetched, Polarized Light).

observed immediately behind the tensile fracture surface as seen in Fig. 7(a). Finally at pressures above the BDTP, cleavage was suppressed and the specimens failed by rupture, (Fig. 7b). The evidence of mechanical twins is less and even in view of the large plastic strains, the grains are equiaxed. This is indicative that the high strains were sufficient to cause post test recrystallization prior to metallographic preparation.

Tin–bismuth alloys

The trend in ductility exhibited by various Sn–Bi alloys compositions at atmospheric pressure and the variation in transition pressure of these compositions is shown in Fig. 8. Ductility is seen to be a maximum for pure tin and for near-eutectic compositions with small Bi additions severely lowering the ductility of the high Sn alloys. Comparison of the two curves shows a direct relationship to exist between the effects of pressure and composition on ductility. Those areas having high ductility (pure Sn and near-eutectic compositions) correspond to the low transition pressures, and compositions having a low inherent ductility required a higher value of superimposed hydrostatic pressure in order to fail by rupture.

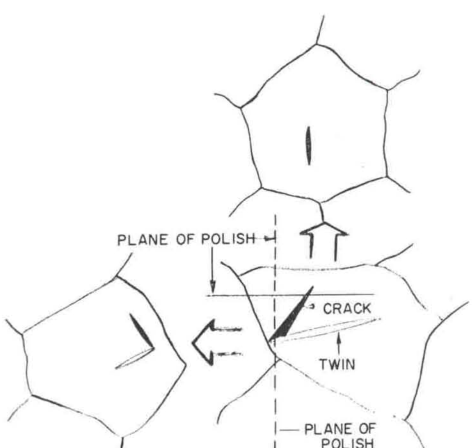

FIG. 6. A schematic representation of the appearance of cracks without metallographically observed obvious means of nucleation. The plane of polish intersects the crack above the point of nucleation, and results in the structures seen in Fig. 5(b).

90 *per cent* Sn–bal Bi *alloy*

For specimens of 90 per cent Sn–bal Bi tested to failure at atmospheric pressure, failure occurs along a section nominally perpendicular to the longitudinal axis; as the pressure increases, the appearance of the fracture corresponds to failure by ductile rupture. At atmospheric and low values of superimposed hydrostatic pressure, cracks are seen to originate along the interface between Bi particles and the Sn matrix (Fig. 9), whereas particle–matrix separation is not seen in specimens tested closer to the BDTP. Numerous voids, having the general shape of microcracks, were seen in areas adjacent to the fracture surface at atmospheric and near-atmospheric pressures (Fig. 10a), but not at pressures approaching the BDTP (Fig. 10b). At atmospheric and low pressures, the mode of fracture appears to be mixed, with evidence for the occurrence of both cleavage at interphase boundaries and ductile tearing present as seen in Fig. 11(a). As the superimposed hydrostatic pressure approaches the BDTP, the fracture surface gradually converts to a dimpled structure, Fig. 11(b), with these dimples decreasing in size at the BDTP as shown in Fig. 11(c).

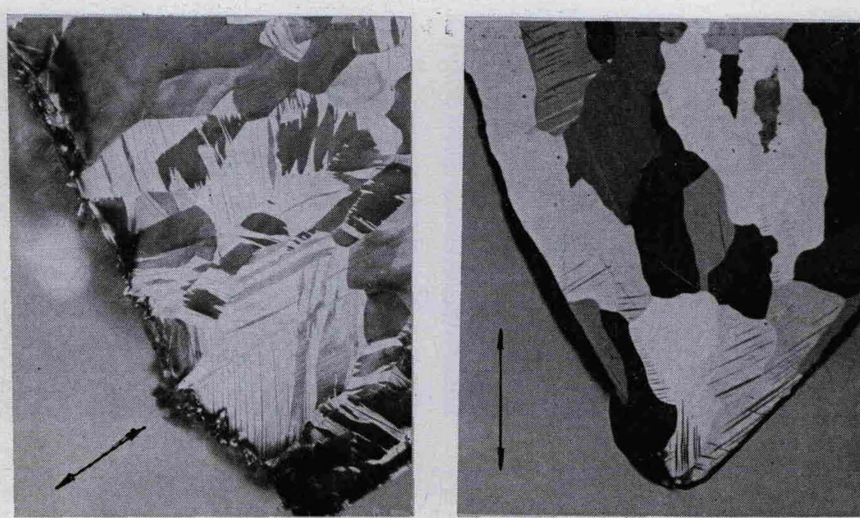

FIG. 7. The microstructure of pure bismuth specimens which fractured at superimposed hydrostatic pressures of: (a) 6.3×10^8 N/m^2, and (b) 14.2×10^8 N/m^2. 50×, Unetched, Polarized Light. Tensile axis indicated by arrows.

75 *per cent* Sn–bal Bi *alloy*

As compared to the former alloy, this alloy contains a higher density of bismuth particles along the Sn grain boundaries and crystallographic planes. This results in a higher microcrack density and a greater propensity towards cleavage fracture. The changes with pressure are otherwise effectively the same.

42 *per cent* Sn–bal Bi *alloy*

This near eutectic alloy composition was seen to contain voids in the interior of the specimen behind the fracture surface when tested to failure at atmospheric pressure (Fig. 12a). Of interest is the shape of the voids; the "V" shape indicates failure by shear,

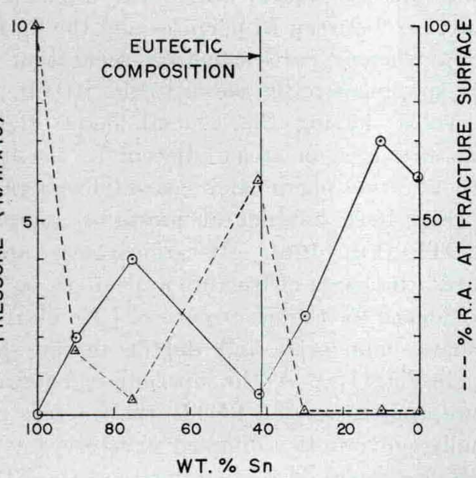

FIG. 8. The variation in ductility and ductility transition pressure as a function of composition.

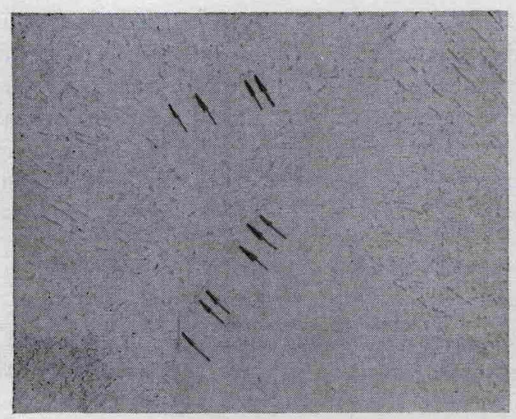

FIG. 9(a). The microstructure of a 90% Sn–bal Bi specimen where pressure at fracture equalled 0.5×10^8 N/m^2. Note the grain size and cracks between matrix and particles straddling grain boundaries. 500×, Unetched.

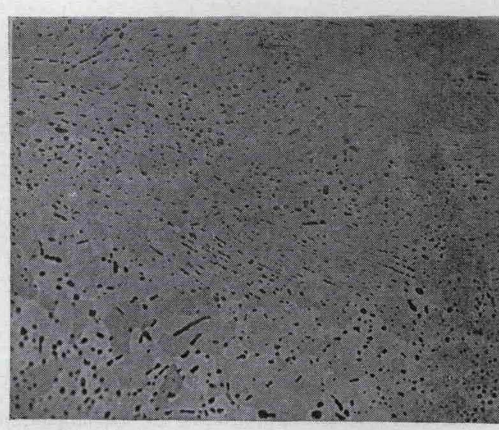

FIG. 9(b). The microstructure of a 90% Sn–bal Bi specimen where pressure at fracture equalled 1.55×10^8 N/m^2. Note the smaller grain size than that shown by Fig. 9 (a) and lack of particle-matrix separation. 500×, Unetched.

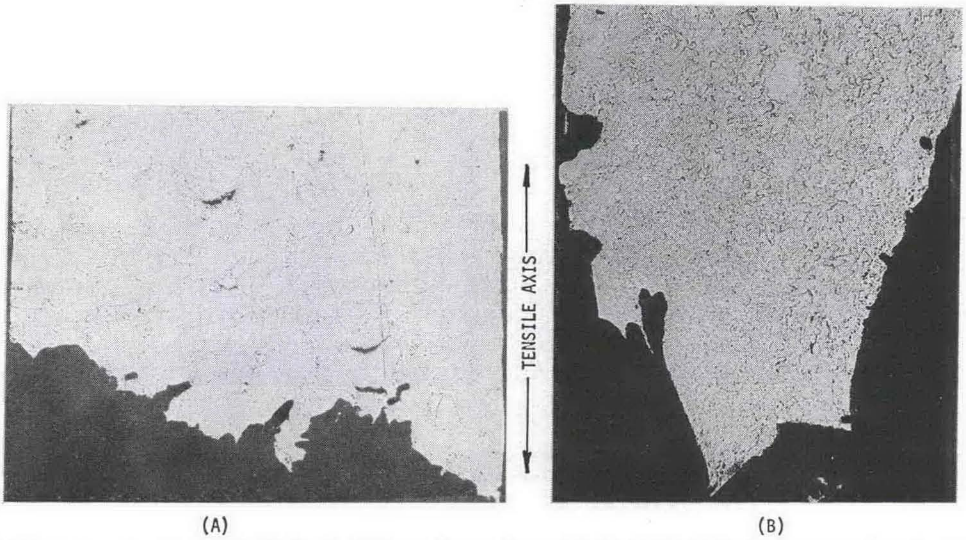

FIG. 10. The microstructure of 90% Sn–bal Bi specimens immediately behind the fracture surface in specimens tested to failure at: (a) atmospheric pressure, and (b) 1.5×10^8 N/m^2. 50×, Etched.

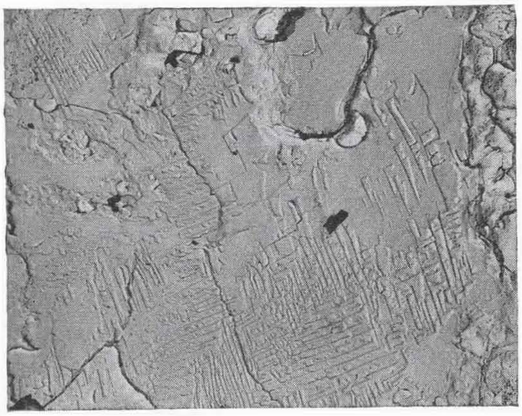

FIG. 11(a). An electron fractograph of a 90% Sn–bal Bi specimen which fractured at 1.05×10^8 N/m^2. Evidence of both ductile fracture and cleavage is seen, with cleavage apparently following the interface between the Sn matrix and Bi particles which precipitated along crystallographic planes, 3250×.

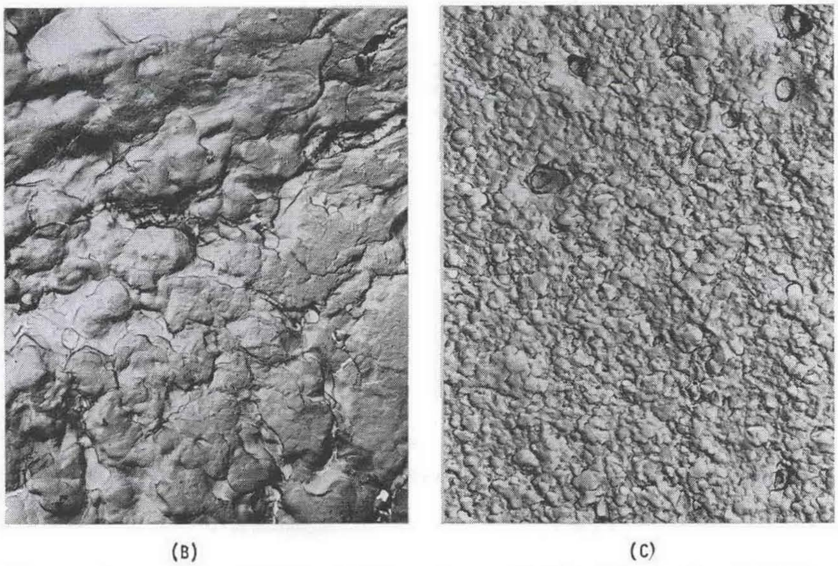

FIG. 11(b), (c). Electron fractographs of 90% Sn–bal Bi specimens which had fractured at (b) 1.55×10^8 N/m^2 and (c) 8.2×10^8 N/m^2 showing a dimpled structure typical of ductile fracture. 3000×.

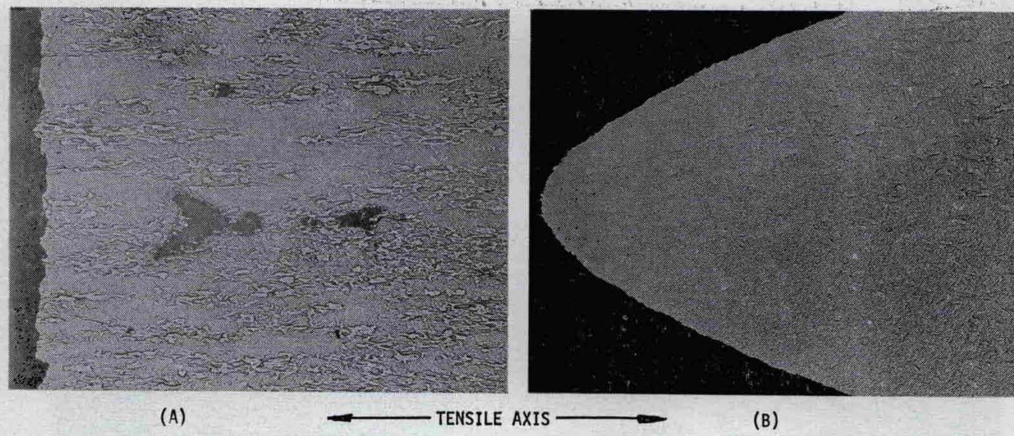

FIG. 12(a), (b). The microstructure of 42% Sn–bal Bi specimens tested to failure at: (a) Atmospheric pressure, showing void formation along the approximate centerline of the specimen. 50 ×, Etched. (b) 4.3×10^8 N/m^2, showing ultimate fracture to occur by rupture. 50 ×, Etched.

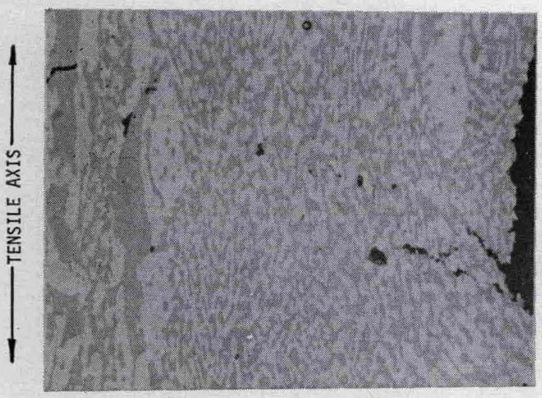

FIG. 12(c). The microstructure of a 42% Sn–bal Bi specimen tested to failure at 1.5×10^7 N/m^2. Numerous instances of voids occurring at particle-matrix interfaces and evidence of cracking of Bi-rich particles are seen. 500 ×, Unetched.

and yet the ultimate fracture is along a plane perpendicular to the longitudinal axis. Figure 12(c) shows cracks initiating within Bi particles, and their link-up through the matrix at the edge of the specimen This behavior allows the fracture surface to exhibit macroscopic features typical of brittle fracture even though the alloy is relatively ductile. Figure 12(b) contrasts the appearance of specimens tested to fracture above the BDTP to those fractured at atmospheric pressure (Fig. 12(a)). Here, failure is by rupture with no voids absberved along the gauge length.

9 *per cent* Sn–bal Bi *alloys*

Specimens containing a high percentage of primary Bi (i.e. hypereutectic alloys) failed by cleavage within the Bi and ductile failure in the Sn at values of superimposed hydrostatic pressure below the BDTP (Fig. 13) and by rupture at pressures above the BDTP (Fig. 14(a)). Also observed was a change in microstructure in regions of the specimens which had undergone more than minimal deformation prior to fracture. The microstructure shown in Fig. 13 and the post deformation zone area of Fig. 14(b) is representative of the microstructure of this composition, with the Bi grain structure resulting from preferred grain orientation. This "oriented" structure of Bi grains within the primary Bi stringers was destroyed in areas adjacent to the fracture surface (Fig. 14a), and clearly indicated the apparent boundary between deformed and underformed material shown in Fig. 14(b). The final grain structure of these deformed areas was not resolved, an effect felt to be due to recrystallization of these same areas.

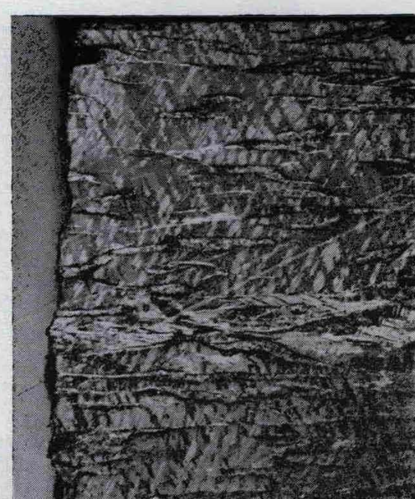

FIG. 13. The microstructure of 9% Sn–bal Bi specimens tested to failure at atmospheric pressure, 50 ×, Unetched, polarized Light.

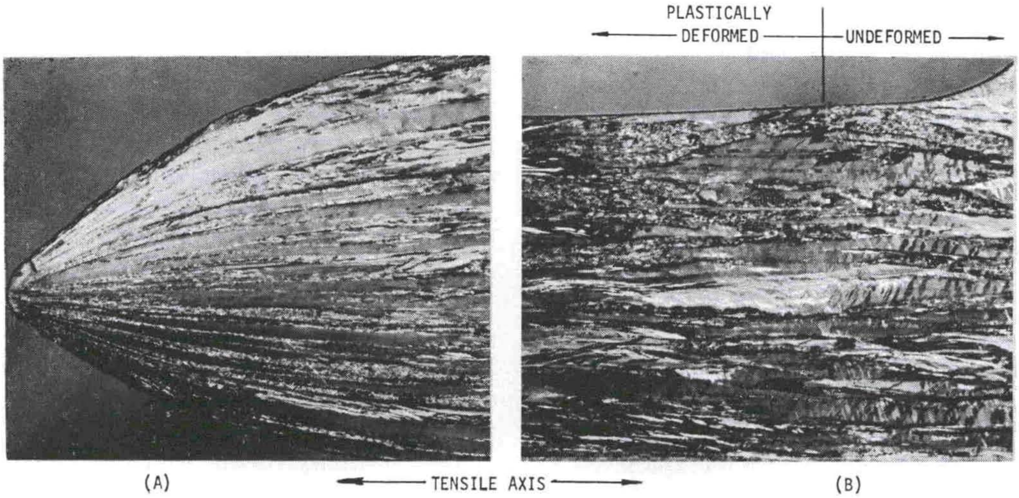

FIG. 14. The microstructure of 9% Sn–bal Bi specimens tested to fracture at 15.0×10^8 N/m^2: (a) showing failure by rapture, 59×, Unetched, Polarized Light. (b) same specimen as in (a) above, but area shown is of material in the vicinity of the shoulders. Note to transition from an indistinct to a pronounced grain structure at the apparent boundary between plastically deformed and undeformed material, 50×, Unetched, Polarized Light.

DISCUSSION

Ductility at atmospheric pressure

Inherent ductility at ambient temperatures and atmospheric pressure is 100 per cent for pure tin and virtually zero for pure bismuth. As an initial assumption, it would appear reasonable that ductility would be some continuous function, decreasing as the volume fraction of Bi is increased. In contrast, the alloy system behaves in a manner quite different from that expected.

In previous work with tin–binary alloys having up to 20 wt.% Bi, Alden[11] noted that specimens were somewhat brittle when annealed at 75–100°C, which he attributed to the embrittling effect of Bi particles along grain boundaries. It was observed in this current study that considerable Bi precipitation also occurred along specific crystallographic planes of the Sn phase. The low ductility of Sn rich alloys is a manifestation of the presence of these Bi particles and results in the following fracture sequence. First, particle–matrix separation occurs along favorably oriented grain boundaries. As the tensile stress is increased, these separations join to form an intergranular crack. Further propagation then occurs by either further grain boundary fracture or (more probably) by travel along a favorably oriented collection of precipitate particles situated along some crystallographic plane in the tin. Eventual link-up of cracks to form the macroscopic fracture surface would be accomplished by the rupture of "bridges" of Sn-rich solid solution. The decrease in ductility with increasing Bi concentration in the Sn-rich alloys is attributed to the closer spacing of the Bi particles, which results in a more continuous plane of weakness.

As the composition is changed so as to approach the eutectic composition, a substantial rise in ductility is observed. This rise, which is on the order of 40 per cent, appears to be due to a decrease in grain size. Grain size was determined through linear intercept methods, and the average grain diameter of the 90 per cent Sn alloy was approximately 1.2×10^{-1} cm. In the eutectic structure, the interphase distance was approximately 7.6×10^{-5} cm. The difference in grain size (which is of several orders of magnitude) is considered the primary contributing factor for the disparity. Crack initiation occurs by both the cleavage fracture of the Bi and failure at the Sn–Bi interface. However, even though there are more available initiation sites in eutectic vs the Sn-rich alloys, the mean free path before the cracks encounter the ductile Sn phase is much less. Thus, more strain is required to extend cracks through the Sn.

The rapid drop in ductility at Bi levels above the eutectic composition results from the controlling effect of large areas of the brittle Bi phase.

The most probable mechanism for crack nucleation is the intersection of twins with grain boundaries (i.e. the same mechanism as observed in pure bismuth), with a possible assist from grain boundary sliding, as $T = 0.93T_m$. Although evidence of cavity formation along grain boundaries is indicative of grain boundary sliding, none were seen, and rarely was metallographic evidence of separation along grain boundaries observed. This lack of evidence leads to the opinion that grain boundary sliding is a minor mode of crack nucleation, and the predominant mechanism to be the nucleation of cracks at the intersections of twins and grain boundaries.

Effects of superimposed hydrostatic pressures

Ductility in terms of reduction in area as a function of pressure at ambient temperatures is shown for pure Bi and Sn–Bi alloys in Figs. 2(a) and (c). While data reported by Pugh[4] appears to show equivalent levels of ductility to occur at lower pressures, the data given was for a Bi–Ag alloy rather than for pure Bi. The anomalous behavior of Sn–Bi alloys as reported by Livshits *et al*,[10] which was ascribed to the character of the pressure-melting temperature curve for this alloy[14] was not duplicated. However, due to the sensitive response of ductility with composition observed to occur for this alloy system (Fig. 8), small composition differences, which would be present in the cast alloys used by Livshits *et al.*[10] in their investigation, could allow their observed shifts in ductility to occur.

Superimposed hydrostatic pressure will not affect the initiation stage of cleavage fracture except in a small if not negligible way.[15] However, if the effect of a superimposed pressure were to result in counteracting (i.e. decrease) the normal stress by the magnitude of the pressure, crack propagation would be impaired.[7] This would effectively retard intergranular fracture and cleavage. It is apparent from examination of Fig. 7(a) that concomitant with an increase in pressure is an increase in the number of twins and a decrease in the number of cracks observed. It is proposed that the retarding of crack propagation by the application of a superimposed hydrostatic pressure will result in the increase in ductility observed by allowing deformation by twinning to proceed to an extent not possible at atmospheric pressure. Also, there exists in the literature some evidence for the enhancement of deformation of bismuth by slip and grain boundary sliding when exposed to superimposed hydrostatic pressure.[16]

Also, an effect of pressure would be to collapse voids forming on a microscopic scale. Since the pressure to collapse a void in a given material is given as approximately two-thirds the yield strength[12] of the material and the tensile strength of tin is given[13] as $1.4 \times 10^4 \mathrm{N/m^2}$ (2100 psi), it would be expected that pressure would have a strong effect on the formation, growth and coalescence of voids in the Sn matrix. Fractographs, Figs. 14(b) and (c), taken at the apparent ultimate fracture surface show dimpling, with the size of dimples decreasing and the frequency of occurrence increasing as the pressure increases, indicating that the effect of pressure will be to reduce void growth, probably by reducing the rate of vacancy diffusion coupled with the tendency to collapse voids at pressures equal to two-thirds the yield stress and to decrease the normal stress contributions to fracture which would tend to promote failure by mechanisms dependent on shear strain.

It should be noted that the value for the BDTP for pure bismuth $6.5 \times 10^8 \mathrm{N/m^2}$ (6.5 kb) is approximately $2 \times 10^8 \mathrm{N/m^2}$ (2 kb) higher than a value for the BDTP derived from results reported by Pugh for a bismuth 2 per cent silver alloy[9] and is taken as an indication of the sensitivity of the BDTP to impurity levels. Also of note is the shifting of the BDTP to $11.5 \times 10^8 \mathrm{N/m^2}$ (11.5 kb) for the as-received (as cast) materials, which is taken to indicate the effects of microstructure (columnar vs equiaxed) and possible casting defects (such as internally oxidized areas etc.), in addition to any chemical effects introduced by the remelting and subsequent extrusion. It is readily apparent that parameters describing the initial conditions with respect to purity and structure would have a large effect on subsequent mechanical behavior.

While twinning is recognized as the predominant mode of deformation at atmospheric pressure,[17,18] the suggestion by Davidson *et al.*[7] that superimposed hydrostatic pressure will affect the normal stress component of the basic Griffith relationship[19] by decreasing the normal tensile stress by the magnitude of the pressure, thereby impairing or suppressing crack propagation by cleavage or intergranular modes, is considered to be especially relevant for pure bismuth as bismuth obeys a critical normal stress to fracture law.[20] Therefore, since the propagation of microcracks would be suppressed by application of a superimposed hydrostatic pressure, the propensity towards deformation by twinning should be enhanced, giving rise to an increase in ductility. At pressures greater than $5 \times 10^8 \mathrm{N/m^2}$ (5 kb), grain boundary effects and slip have been observed in pure Bi.[16,21] It is quite possible that the effect of pressure on the deformation characteristics of bismuth, when combined with the effect on the normal tensile stress component and subsequent effects on crack propagation, gives rise to the abrupt ductile–brittle transition observed.

The ductility response of Sn–Bi alloys subjected to superimposed hydrostatic pressures is considered to be a manifestation of the shift of the brittle-to-ductile transition temperature (BDTT). However, at or near atmospheric pressure, this effect may not be seen as it may be masked by recrystallization or high temperature ($>0.5T_m$) rupture phenomena.

CONCLUSIONS

1. The brittle-to-ductile transition pressure for pure (99.999 per cent) bismuth is approximately $6.5 \times 10^8 N/m^2$ (6.5 kb) and is a sharp rather than gradual transition. The transition is sensitive to grain size, with the transition pressure increasing with the grain size.

2. Fracture in pure bismuth occurs by trans-granular cleavage, and is nucleated at the inter-section of twins and grain boundaries.

3. The effect of a superimposed hydrostatic pressure is to suppress fracture propagation, and enhance the operation of mechanisms of deformation (i.e. slip and twinning) and ductile fracture.

4. The low ductility of Sn–Bi alloys having a small volume fraction of Bi is due to fracture nucleating by the separation of the Sn matrix from the Bi particles situated along the grain boundaries and propagating crystallographic planes. The ductility of hypereutectic Sn–Bi alloys is controlled by the fracture behavior of primary bismuth.

5. The brittle-to-ductile transition of Sn–Bi alloys exposed to a range of superimposed hydrostatic pressures is a logical consequence of a temperature induced brittle-to-ductile transition.

ACKNOWLEDGEMENTS

The authors would like to acknowledge financial support of this project by the Army Materials and Mechanics Research Center, and the able assistance and skill of Ms. Theresa Brassard in the metallography of the pure materials and alloys used, and Messrs. Leo MacNamara and Harry Nazarian for their aid in electron fractography and the conduct of experiments.

REFERENCES

1. P. W. Bridgman, *Research* (Lond.) **2**, 550 (1949).
2. P. W. Bridgman, *J. appl. Phys.* **24**, 560 (1953).
3. B. I. Beresnev, L. F. Vereshagin, Yu. N. Ryabinin and L. D. Livshits, *Some Problems of Large Plastic Deformation of Metals at High Pressures*. Translation by V. M. Newton. Macmillan, New York (1963).
4. H. Ll. D. Pugh, *1st Int. Conf. on Metals*, Phils. pa. (1964).
5. A. Bobrowsky, *ASME Annual Winter Mtg.*, N.Y. Nov. 29–Dec. 4 (1964).
6. J. R. Galli and P. Gibbs, *Acta Met.* **12**, 775 (1964).
7. T. E. Davidson, J. C. Uy and A. P. Lee, *Acta Met.* **14**, 937 (1966).
8. M. Brandes, *The Mechanical Behavior of Materials Under Pressure*, edited by H. Ll. D. Pugh, Chap. 6, Elsevier, New York (1970).
9. H. Ll. D. Pugh, *Symposium on Irreversible Effects of High Pressure and Temperature on Materials*. A.S.T.M. February 1964, Special Technical Publication No. 374.
10. L. D. Livshits, B. I. Beresnev and Yu. N. Ryaginin, *Nauk, SSSR*, **161**, (5), 1077 (1965).
11. T. H. Alden, *Acta Met.* **15**, 469 (1967).
12. O. Hoffman and G. Sachs, *Introduction to the Theory of Plasticity for Engineers*, pp. 69–74. McGraw-Hill, New York (1953).
13. *Metals Handbook*, 8th ed. (1961).
14. E. G. Poniatowsky, *Fiz Metal, i Metalloved* **16**, 622 (1963).
15. D. Francois and T. T. Wilshaw, *J. appl. Phys.* **39** (9), 4170 (1968).
16. T. E. Davidson and C. G. Homan, *Trans. AIME* **227** (1), 167–176 (1963).
17. H. J. Gough and H. L. Cox, *J. Inst. Metals* **48**, 227 (1932).
18. W. F. Berg and F. D. Startoff, *Nature* **136**, 915 (1935).
19. A. A. Griffith, *Proc. 1st Int. Cong. Appl. Mech.* pp. 55, Delft (1924).
20. M. Georgieff and E. Schmid, *Z. Phys.* **64**, 845 (1930).
21. T. E. Davidson, J. C. Uy and A. P. Lee, *Trans. AIME* **233**, 820 (1965).